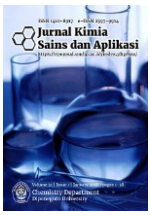
ISSN: 1410-8917
Jurnal Kimia Sains & Aplikasi
e-ISSN: 2597-9914

Jurnal Kimia Sains dan Aplikasi 29 (8) (2026): 559-567

Jurnal Kimia Sains dan Aplikasi
Journal of Scientific and Applied Chemistry

Journal homepage: http://ejournal.undip.ac.id/index.php/ksa



Green-Synthesised Silver Nanoparticle–Loaded Sodium Alginate Beads Using *Asplenium nidus* for Potential Antibacterial and Hg^{2+} Ion Sensing Applications

Doni Notriawan [1,*], Eka Angasa [2], Reza Pertiwi [3], Zavira Nurjali [1], Meiliana Ngasti Wati [1]

[1] Science Laboratory, Faculty of Mathematics and Natural Sciences, Universitas Bengkulu, Jalan WR. Supratman, Kendang Limun, Kota Bengkulu 38371, Indonesia
[2] Department of Chemistry, Faculty of Mathematics and Natural Sciences, Universitas Bengkulu, Jalan WR. Supratman, Kandang Limun, Kota Bengkulu 38371, Indonesia
[3] Department of Pharmacy, Faculty of Mathematics and Natural Sciences, Universitas Bengkulu, Jalan WR. Supratman, Kandang Limun, Kota Bengkulu 38371, Indonesia

* Corresponding author: doninotriawan@unib.ac.id

https://doi.org/10.14710/jksa.29.8.559-567

Article Info

Article history:

Received: 05th June 2026
Revised: 31st August 2026
Accepted: 22nd September 2026
Online: 30th September 2026

Keywords:
Asplenium nidus; Silver Nanoparticles; Nanocomposite; Antibacterial

Abstract

Silver nanoparticles (AgNPs) have attracted considerable interest due to their antibacterial properties and potential for metal-ion sensing. This study aimed to develop sodium alginate/silver nanoparticle (SA/AgNPs) beads using *Asplenium nidus* leaf extract and evaluate their antibacterial activity and colourimetric response toward Hg^{2+} ions. AgNPs were biosynthesised using *Asplenium nidus* leaf extract and incorporated into a sodium alginate matrix to form SA/AgNPs nanocomposite beads. The formation of AgNPs was indicated by a colour change from clear yellow to brown and confirmed by UV–Vis absorption in the range of 420–450 nm. The resulting SA/AgNPs nanocomposite beads exhibited antibacterial activity against *Escherichia coli*, producing an inhibition zone of approximately 1 mm, whereas sodium alginate beads without AgNPs showed no inhibition zone. In addition, the SA/AgNPs nanocomposite beads exhibited a concentration-dependent visual response toward Hg^{2+} ions (10–80 ppm), with a distinct colour change from brown to white, while the beads exposed to demineralised water remained brown after 24 h. These findings demonstrate that *Asplenium nidus* leaf extract can facilitate the biosynthesis of AgNPs and that the resulting SA/AgNPs nanocomposite beads exhibit both antibacterial activity and a visible response toward Hg^{2+} ions. The combination of a plant-mediated synthesis approach and alginate-based bead fabrication provides a simple platform with potential for antibacterial applications and preliminary colourimetric detection of Hg^{2+} ions.

1. Introduction

Silver nanoparticles (AgNPs) are one of the metal-based nanomaterials that have been studied most extensively because of their wide range of applications, especially in the field of biomedicine [1, 2, 3, 4]. Many studies have shown that AgNPs are effective as antimicrobial agents, for example, in wound treatment, where topical preparations containing silver nanoparticles have been widely used for treating infections in open wounds [5]. Because of their ability to act against a broad spectrum of microorganisms, AgNPs are effective against a wide variety of microbes, including pathogenic bacteria [6]. In addition to their use as antibacterial agents, AgNPs have attracted considerable attention as sensing materials for heavy metal ions, particularly mercury (Hg^{2+}) [7, 8]. Mercury is a highly toxic heavy metal that presents serious hazards to both human health and the environment, even at low concentrations [9]. AgNPs have a strong affinity for Hg^{2+} ions as a result of Ag–Hg interactions [10], and this causes a change in the surface plasmon resonance of the

AgNPs, with the result that a visible colour change occurs [11].

In recent years, there has been a growing focus on environmentally friendly techniques for synthesising AgNPs, commonly referred to as green synthesis. This approach utilises biological reducing agents derived from plant extracts and offers several advantages, including simplicity, cost-effectiveness, and reduced environmental impact [4, 12, 13]. A number of plant species have been used, such as *Hibiscus syriacus* [14], *Vitex altissima* [15], *Bacopa monnieri* [16], and *Brucea javanica* (L.) Merr [17]. Plant biomolecules such as proteins, amino acids, organic acids, vitamins, and secondary metabolites, including flavonoids, alkaloids, polyphenols, terpenoids, heterocyclic compounds, and polysaccharides, have an important role in the reduction of metal ions and in the stabilisation of the nanoparticles [18].

Even though AgNPs have promising antibacterial properties, a major drawback is their tendency to aggregate, especially upon contact with bacterial cells. This aggregation leads to a reduction in specific surface area and, as a result, decreases their antibacterial activity [19]. To address this drawback, AgNPs are typically incorporated into polymer-based composite systems, which serve as stabilising matrices, preventing aggregation and improving dispersion. A number of biocompatible polymers, such as chitosan, polyvinyl alcohol, cellulose, and gelatin, have been widely investigated for this application. Earlier studies have shown that chitosan–silver nanoparticle composite films display increased antibacterial activity as a result of better nanoparticle stability and greater surface interaction with bacterial cells [20, 21, 22].

Alginate is a natural polysaccharide composed of β-D-mannuronic acid and α-L-guluronic acid, and is well known for its biocompatibility, biodegradability, and good gel-forming properties. Because of these features, it can be used as a matrix for nanoparticle-based composites [23, 24]. Earlier research has described alginate–silver nanoparticle nanocomposites for the colourimetric detection of Hg^{2+} ions [25]. In those studies, though, the AgNPs were produced by chemical reduction with sodium borohydride ($NaBH_4$), which has led to concerns regarding environmental safety and sustainability.

Asplenium nidus is a fern commonly found in tropical rainforests, including the Bengkulu region. Despite its widespread occurrence, it remains underutilised by local communities and is often regarded as an undesirable plant. However, the leaves of *Asplenium nidus* contain a number of secondary metabolites, including flavonoids, tannins, polyphenols, and saponins [26], which may contribute to the reduction and stabilisation of AgNPs during green synthesis. In the present study, an extract from *Asplenium nidus* leaves was used as a natural means of synthesising AgNPs, with the resulting nanoparticles then incorporated into sodium alginate to produce SA/AgNP beads. The main innovation of this study lies in combining a plant-mediated synthesis method with the production of alginate beads to obtain a material that exhibits both antibacterial properties and a visible response to Hg^{2+} ions. This method differs from earlier alginate–AgNP systems, which generally use chemically synthesised AgNPs. The SA/AgNPs nanocomposite beads were tested against *Escherichia coli*, and their colour response was examined at various Hg^{2+} concentrations. The results offer a simple and environmentally sound way of preparing multifunctional silver-based beads with potential applications in antibacterial applications and in the initial visual detection of Hg^{2+} ions.

2. Experimental

2.1. Materials

The materials used in this study were *Asplenium nidus* leaves collected from a forest in Bengkulu, $AgNO_3$ (Merck, analytical reagent grade), $CaCl_2$ (food grade), sodium alginate (SA; food grade), demineralized water, $HgCl_2$ (Merck, analytical reagent grade), $SnCl_2{\cdot}2H_2O$ (tin(II) chloride dihydrate; Merck, analytical reagent grade), and $Pb(CH_3COO)_2{\cdot}3H_2O$ (lead(II) acetate trihydrate; Merck, analytical reagent grade).

The AgNPs were characterised using a UV–Vis spectrophotometer (SPECTROstar Nano, BMG LABTECH) and transmission electron microscope (TEM; JEM-1400). The nanocomposite beads were characterised using a Fourier-transform infrared spectrophotometer (FTIR; Bruker, Germany), scanning electron microscope (SEM; FEI Quanta 650), and X-ray diffractometer (XRD; PANalytical AERIS).

2.2. Biosynthesis of AgNPs Using *Asplenium nidus* Leaf Extract

AgNPs were biosynthesised according to the method described by Sati *et al.* [1]. The biosynthesis process was initiated by preparing the *Asplenium nidus* leaf extract. Briefly, 4 g of fresh *Asplenium nidus* leaves were added to 100 mL of demineralised water and heated at 70°C for 30 min. The resulting extract was then filtered, and the filtrate was used as the reducing and stabilising agent for the synthesis of AgNPs. The filtrate was mixed with 0.01 M $AgNO_3$ at various volume ratios of 1:3, 1:4, 1:5, 1:6, and 2:3. The reaction mixtures were stirred under ambient light conditions, and the formation of AgNPs was indicated by a visible colour change.

2.3. Characterisation of AgNPs

The formation of AgNPs was confirmed using a UV–Vis spectrophotometer by recording the absorption spectrum of the AgNP colloidal suspension over the wavelength range of 200–800 nm. The characteristic surface plasmon resonance (SPR) absorption band of AgNPs was expected to occur at approximately 410–430 nm. The morphology and particle size of the synthesised AgNPs were examined using TEM.

2.4. Preparation of SA/AgNPs Nanocomposite Beads

The alginate/silver nanoparticle (SA/AgNPs) nanocomposite beads were prepared following a previously reported method with some modifications [27]. Sodium alginate (1.0 g) was dissolved in 25 mL of

colloidal AgNPs synthesised using *Asplenium nidus* leaf extract. The resulting mixture was loaded into a 10-mL syringe and extruded dropwise into a 2% $CaCl_2$ solution under slow stirring with a magnetic stirrer. After bead formation, the suspension was continuously stirred for 30 min to facilitate the crosslinking process [28]. The resulting nanocomposite beads were separated from the 2% $CaCl_2$ solution using a sieve and rinsed with demineralised water.

2.5. Characterisation of SA/AgNPs Nanocomposite Beads

The functional groups of the SA/AgNPs nanocomposite beads were identified using FTIR spectroscopy to evaluate changes associated with AgNP incorporation. The morphology of the nanocomposite beads was examined using SEM at an accelerating voltage of 10.00 kV and a magnification of 800×. Energy-dispersive X-ray spectroscopy (EDS) was performed in conjunction with SEM to determine the elemental composition of the nanocomposite beads and verify the presence of silver. The crystalline phases of the nanocomposite beads were analysed using XRD with Cu Kα radiation at 40.0 kV and 15.0 mA over a 2θ range of 5.003–90.000°, with a step size of 0.0217°.

2.6. In Vitro Antibacterial Activity of SA/AgNPs Nanocomposite Beads

The target bacteria used in this study were *Escherichia coli* ATCC 8739 and *Staphylococcus aureus*. A colony of each bacterial strain was inoculated into Trypticase Soy Broth (TSB) and incubated in a shaking incubator at 37°C for 24 h. Subsequently, 1 mL (1%, v/v) of each bacterial suspension was inoculated into 100 mL of molten Trypticase Soy Agar (TSA) medium. The mixture was homogenised using a magnetic stirrer for 2 min and then poured into sterile Petri dishes. After the TSA medium solidified, the treatment samples were placed onto the agar surface containing the target bacteria. The plates were then incubated at 37°C for 24 h. The antimicrobial activity of the treatment was evaluated based on the formation of a clear inhibition zone around the treatment sample.

2.7. Evaluation of SA/AgNPs Nanocomposite Beads in Hg^{2+} Ion Solutions

The sensing performance of SA/AgNPs nanocomposite beads was evaluated by immersing the beads in aqueous solutions containing Hg^{2+} ions and monitoring the resulting colour changes. The beads were exposed to Hg^{2+} solutions at concentrations of 10, 20, 40, 60, and 80 ppm to assess their sensitivity. The visual response to each Hg^{2+} concentration was observed and recorded after 30 min and 24 h of exposure to evaluate the concentration- and time-dependent colour changes. In addition, selectivity tests were conducted by immersing the SA/AgNPs nanocomposite beads in Sn^{2+} and Pb^{2+} ion solutions at a concentration of 100 ppm.

3. Results and Discussion

3.1. Biosynthesis of AgNPs Using *Asplenium nidus* Leaf Extract

The biosynthesis of AgNPs was carried out using $AgNO_3$ as the precursor and *Asplenium nidus* leaf extract as a bioreductant at a concentration of 4%. During the reaction, a visible colour change from transparent yellow to brown was observed within 15 min (Figure 1), indicating the formation of AgNPs. This visual observation was further supported by the UV–Vis analysis, which showed characteristic absorption peaks at approximately 440 nm for all biosynthesis variations (Figure 2a). The appearance of these absorption bands in the 410–450 nm region is associated with the SPR of AgNPs, confirming the reduction of Ag^+ to Ag^0 and the formation of nanoscale silver particles. The reduction process is likely mediated by phytochemical constituents present in *Asplenium nidus* leaf extract, including phenolic compounds, flavonoids, tannins, and other polyphenolic molecules containing electron-donating functional groups such as –OH and –COOH [2, 3, 4].

The characteristic brown colouration observed in nanoparticle suspensions is associated with SPR, which originates from the collective oscillation of conduction electrons in silver nanoparticles upon light excitation [4, 7]. The rapid colour transition observed suggests an efficient and environmentally friendly biosynthesis process, highlighting the effectiveness of *Asplenium nidus* leaf extract in mediating the green synthesis of AgNPs.

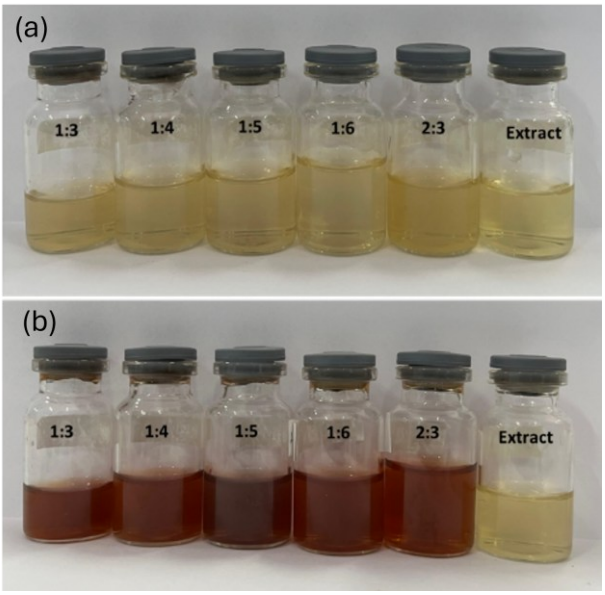


Figure 1. Colour change of the reaction mixture during silver nanoparticle biosynthesis: (a) before the reaction and (b) after 15 min of reaction

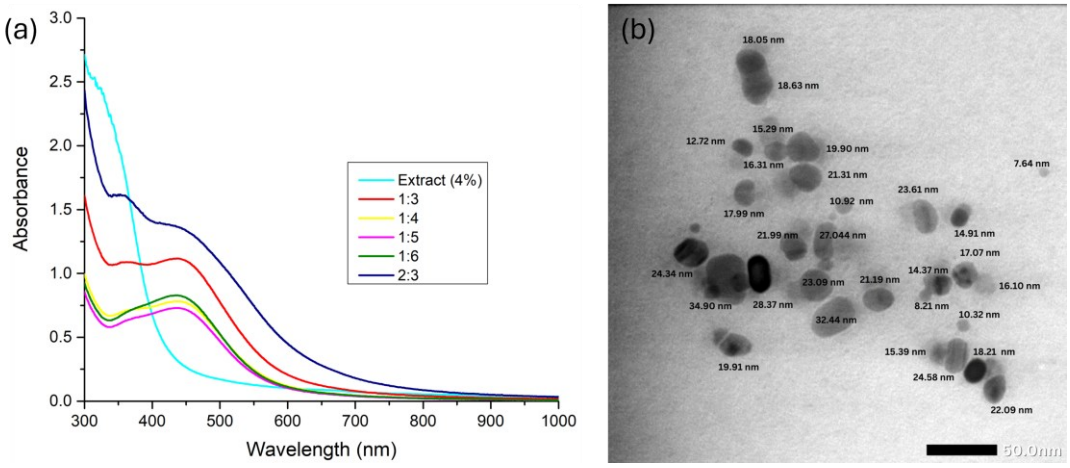


Figure 2. (a) UV–Vis absorption spectra and (b) TEM image of colloidal AgNPs synthesised at a 1:3 ratio using *Asplenium nidus* leaf extract

The experimental UV–Vis results further demonstrate that the biosynthesis conditions influenced the optical response of the AgNPs. Although the absorption maximum remained at around 440 nm, the absorbance intensity varied across the extract-to-$AgNO_3$ ratios (Figure 2a), indicating differences in the amount of dispersed nanoparticles formed under each condition. The consistent position of the SPR band suggests that the synthesised particles maintained a relatively similar optical character, while differences in absorbance intensity may reflect variations in nanoparticle concentration and/or formation yield. These UV–Vis findings are consistent with the observed brown colouration after 15 min (Figure 1), providing complementary visual and spectroscopic evidence for AgNP formation. Thus, rather than relying solely on the theoretical SPR phenomenon, the colour change and absorption characteristics observed in this study demonstrate that *Asplenium nidus* leaf extract effectively mediated the formation of AgNPs under the applied synthesis conditions.

The highest absorbance intensity was observed in the 1:3 biosynthesis variation, suggesting more efficient reduction of Ag^+ ions and a higher production of AgNPs under this condition. Similar relationships between absorbance intensity and nanoparticle concentration have been widely reported in green-synthesised AgNPs systems. Therefore, a 1:3 ratio was chosen as the optimal condition for the subsequent fabrication of alginate-AgNPs beads. This is also supported by the TEM results for AgNPs shown in Figure 2b. TEM analysis confirmed the formation of nanosized AgNPs with relatively similar morphology and varying particle sizes ranging from approximately 7 to 35 nm. The results obtained are consistent with previous studies reporting silver nanoparticles with a nearly uniform spherical morphology and particle sizes in the nanometer range, typically between 9 and 31 nm [8, 9].

3.2. Fabrication of SA/AgNPs Nanocomposite Beads

The SA/AgNPs nanocomposite beads exhibited a brown colouration similar to that of colloidal AgNPs, indicating the successful incorporation and uniform distribution of AgNPs within the alginate matrix while preserving their SPR properties. The beads exhibited a well-defined spherical morphology resulting from ionic gelation between sodium alginate and Ca^{2+} ions, providing structural stability and a homogeneous surface suitable for antibacterial and metal-ion sensing applications. As shown in Figure 3, the FTIR spectrum of SA/AgNPs nanocomposite beads exhibits a wide absorption band of about 3300–3442 cm^{-1}, corresponding to the O–H stretching vibration, a peak of about 1740 cm^{-1} associated with C=O stretching, and a band of about 1600–1628 cm^{-1} associated with asymmetric stretching of the COO^- group in sodium alginate.

Compared to pure SA, only small changes in the position and intensity of the typical bands of O–H and COO^- were observed after AgNP fusion, along with a decrease in band sharpness. These changes indicated a modification of the local chemical environment of the oxygen-containing functional group, likely due to interactions between the silver species and the alginate functional group. The absence of new absorption bands indicates that the main alginate structure was preserved. The spectral changes may therefore reflect weak surface interactions, including electrostatic interactions and coordination, that contribute to silver stabilization in the alginate matrix [10, 11].

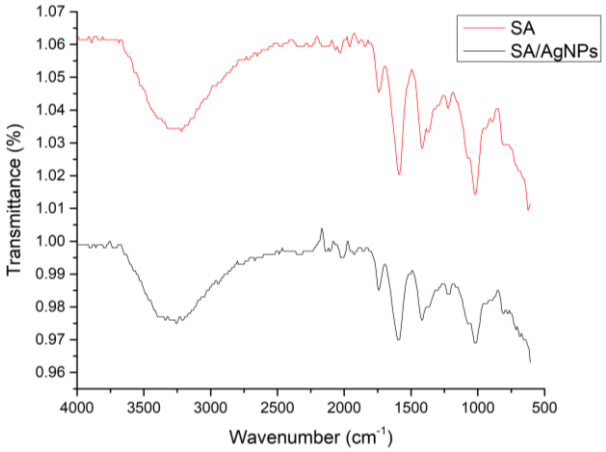


Figure 3. FTIR spectra of SA and SA/AgNPs nanocomposite beads

The characterisation of SA/AgNPs nanocomposite beads using SEM revealed differences between SA and SA/AgNPs. In Figure 4, the surface of pure SA appears relatively rough and inhomogeneous, with a dense polymer matrix and unevenly distributed particle agglomerates. This morphology reflects the natural characteristics of alginate tissues after ionic gelation, in which the polymer structure predominates at the surface in the absence of inorganic fillers.

In contrast, SA/AgNP exhibits significant morphological changes, characterised by a more granular surface and fine particles dispersed throughout the alginate matrix. These small granules are interpreted as AgNPs that are incorporated and distributed relatively homogeneously on the surface and near the surface of the beads. This distribution shows that the process of impregnating AgNPs into the alginate matrix is effective, with alginate acting as a buffering matrix that holds and stabilises the AgNPs. The EDS analysis of the SA/AgNPs nanocomposite beads confirmed the presence of silver (Ag) in the composite, with an Ag content of approximately 16 wt%. The presence of a distinct Ag signal indicates that silver nanoparticles were successfully incorporated into the sodium alginate matrix. The EDS spectrum also showed signals corresponding to the main elements of the alginate matrix, while the relatively high Ag percentage suggests that a substantial amount of silver-containing material was present on the analysed surface.

The XRD pattern of pure SA shows a broad diffraction profile, indicating the predominantly amorphous nature of the polymer matrix (Figure 5). In contrast, the SA/AgNPs nanocomposite beads exhibit several additional and well-defined diffraction peaks at approximately 27.81°, 32.29°, 46.31°, 54.80°, 57.56°, 67.47°, and 76.80° (2θ). These peaks are consistent with the characteristic diffraction pattern of cubic AgCl, corresponding to the (111), (200), (220), (311), (222), (400), and (420) planes, respectively, based on JCPDS No. 31-1238 [12].

The formation of AgCl is likely associated with the use of $CaCl_2$ during bead formation. The Cl^- ions released from the $CaCl_2$ solution can interact with silver species present in the AgNPs-containing material, leading to the formation of AgCl [13]. This phenomenon has also been reported in alginate-based silver composites, where the presence of chloride ions during $CaCl_2$-mediated gelation promoted AgCl formation through the reaction between Ag^+ and Cl^- ions. The appearance of the characteristic AgCl reflections in the XRD pattern of the present SA/AgNPs nanocomposite beads may therefore be associated with the bead-forming process using $CaCl_2$. The broad diffraction profile of SA remains visible, indicating that the predominantly amorphous character of the sodium alginate matrix is retained after bead formation. Thus, the XRD results suggest that the use of $CaCl_2$ during bead formation may contribute to the formation of a crystalline AgCl phase within the SA/AgNPs matrix.

3.3. Antibacterial Testing of SA/AgNPs Nanocomposite Beads

The antibacterial activity of the samples was evaluated against *Staphylococcus aureus* and *Escherichia coli* using the zone-of-inhibition assay, as shown in Figure 6. The results showed a more pronounced antibacterial response against *Staphylococcus aureus* than against *Escherichia coli*. Against *Staphylococcus aureus*, the SA/AgNPs wet beads and AgNPs solution produced an average zone of inhibition of approximately 3.8 mm, whereas the SA/AgNPs dried beads showed a smaller inhibition zone of approximately 2.1 mm.

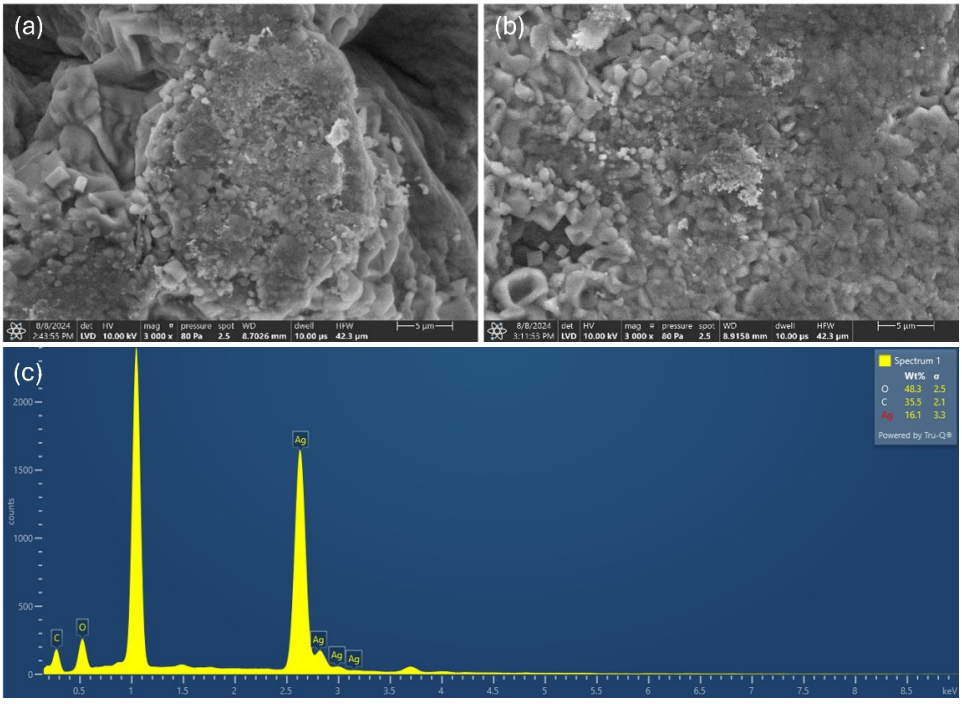


Figure 4. SEM images of (a) SA and (b) SA/AgNPs nanocomposite beads at 5000× magnification and (c) EDS spectrum of the SA/AgNPs nanocomposite beads

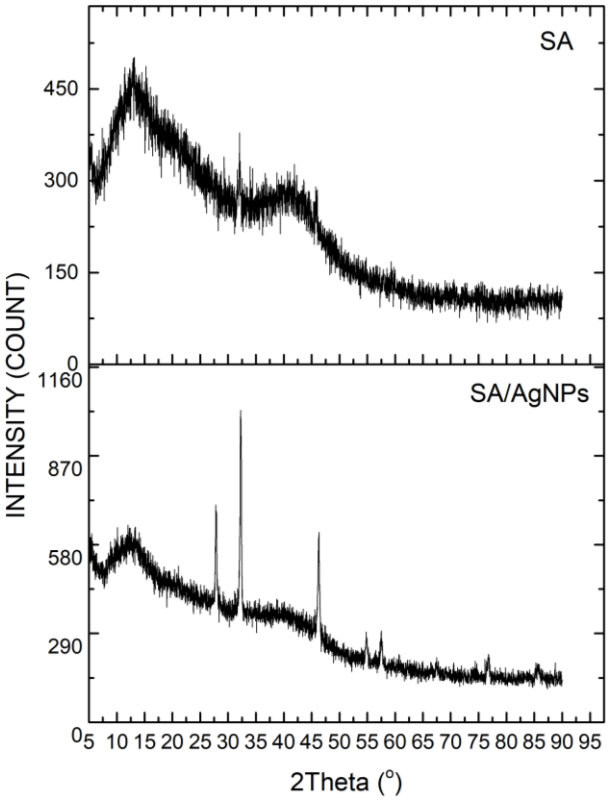


Figure 5. XRD patterns of SA and SA/AgNPs nanocomposite beads

In contrast, the SA wet beads did not produce a detectable inhibition zone, indicating that the antibacterial activity was mainly associated with the presence of AgNPs rather than the alginate matrix itself. The smaller inhibition zone for the dried SA/AgNPs nanocomposite beads compared with the wet beads may be related to differences in the release and diffusion of silver-containing species from the polymer matrix into the agar medium. The positive control produced a substantially larger inhibition zone of approximately 20.3 mm, indicating that the antibacterial activity of the SA/AgNPs samples was considerably lower than that of the reference antibacterial agent. The antibacterial activity of AgNPs has been attributed to several mechanisms, including interaction with the bacterial cell envelope, release of Ag^+ ions, membrane disruption, oxidative stress, and interference with intracellular components [4].

Against *Escherichia coli*, the SA/AgNPs wet beads produced a relatively small inhibition zone of approximately 1.5 mm, while no clear inhibition zone was observed for the SA wet beads, SA/AgNPs dried beads, or AgNPs solution. The weaker response may be related to differences in the cell-envelope structure of the two bacterial species. *Escherichia coli* is a Gram-negative bacterium with an outer membrane containing lipopolysaccharides, whereas *Staphylococcus aureus* is Gram-positive and has a thick peptidoglycan-rich cell wall. These structural differences can influence the interaction of AgNPs and released Ag^+ ions with bacterial cells and consequently affect their susceptibility to silver-based materials [14].

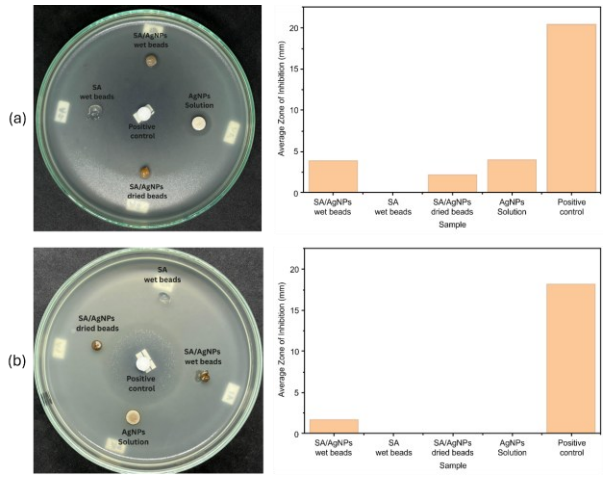


Figure 6. Antibacterial activity and average zone of inhibition of SA/AgNPs wet beads, SA wet beads, SA/AgNPs dried beads, AgNPs solution, and positive control against (a) *Staphylococcus aureus* and (b) *Escherichia coli*

However, the antibacterial response of AgNPs can vary depending on nanoparticle size, surface characteristics, concentration, and bacterial strain, so the difference observed here should be interpreted specifically in the context of the present experimental conditions [15]. Overall, the SA/AgNPs nanocomposite beads exhibited detectable but relatively weak antibacterial activity, particularly against *Staphylococcus aureus*, while their activity against *Escherichia coli* was more limited.

3.4. Qualitative Evaluation of Colourimetric Hg^{2+} Sensing Using Nanocomposite Beads

Figure 7 shows the time-dependent visual response of SA/AgNPs nanocomposite beads upon exposure to Hg^{2+} ion solutions at different concentrations (10–80 ppm), observed after 30 min and 24 h of incubation. A qualitative visual change in colour was observed at different Hg^{2+} concentrations, with more apparent changes at higher concentrations, whereas no noticeable change was observed in the distilled water control. These observations demonstrate the visible colourimetric response of the SA/AgNPs nanocomposite beads toward Hg^{2+} ions.

The observed colour change may be attributed to the redox interaction between Hg^{2+} and metallic Ag^0 in silver nanoparticles. Hg^{2+} has a higher standard reduction potential than the Ag^+/Ag^0 couple, it can oxidise Ag^0 to Ag^+ while being reduced to Hg^0. This alters the surface and optical properties of the AgNPs, changing their characteristic brownish colour. Colourimetric detection of Hg^{2+} using AgNPs has been reported to occur through several possible mechanisms, including complexation-induced aggregation, Ag–Hg alloy formation, and redox reactions. Among these mechanisms, the redox pathway involves the direct reaction between Hg^{2+} and Ag^0, yielding Hg^0 and Ag^+. Previous studies have suggested that this redox mechanism can play an important role in the colourimetric detection of Hg^{2+} using AgNPs, particularly when LSPR band changes occur without typical nanoparticle aggregation [16].



Figure 7. Visual colour change of SA/AgNPs nanocomposite beads in Hg^{2+} solutions at different concentrations, indicating their potential application as a colourimetric Hg^{2+} sensor: (a) 30 min and (b) 24 h



Figure 8. Visual comparison of colourimetric responses of nanoparticle beads to Sn^{2+}, Pb^{2+}, and Hg^{2+} ions

The effect of Hg^{2+} concentration on the visual response of the SA/AgNPs nanocomposite beads was also evident from the gradual increase in colour change with increasing Hg^{2+} concentration. As shown in Figure 7, qualitative visual changes in colour were already observed after 30 min of exposure to Hg^{2+} solutions at different concentrations. At lower Hg^{2+} concentrations, the colour change was less pronounced, whereas more apparent changes were observed at higher concentrations. As the Hg^{2+} concentration increased from 10 to 80 ppm, more Hg^{2+} ions became available to interact with metallic Ag^0 on the nanoparticle surface, promoting the oxidation of Ag^0 to Ag^+. Consequently, the bead colour became progressively paler, and the formation of the white precipitate became more apparent at higher Hg^{2+} concentrations [16].

This qualitative visual response suggests that the extent of the colour change is associated with the concentration of Hg^{2+} interacting with the silver-containing phase, indicating the potential of SA/AgNPs nanocomposite beads as a simple semi-quantitative colourimetric sensor for Hg^{2+} detection. After 24 h, the colour change becomes more pronounced and uniform, suggesting enhanced diffusion of Hg^{2+} ions into the porous alginate matrix and more extensive interaction with immobilised AgNPs. The hydrogel nature of sodium alginate facilitates ion diffusion while maintaining nanoparticle stability, which contributes to consistent and reproducible sensor responses.

The colourimetric detection of Hg^{2+} ions using AgNPs has been previously documented in the literature [17, 18]. This sensing mechanism is mainly driven by a redox interaction between Hg^{2+} ions and metallic silver (Ag^0) located on the AgNP surface. Because the standard redox potential of the Hg^{2+}/Hg^0 couple ($E° = +0.80$ V) is comparable to, yet slightly lower than, that of the Ag^+/Ag^0 couple ($E° = +0.85$ V), Hg^{2+} ions are preferentially reduced, accompanied by the oxidation of surface silver atoms. As a consequence, metallic mercury is generated directly on the surface of the AgNPs [19].

In addition, the alginate matrix plays an important role in immobilising the AgNPs within the bead structure, allowing the silver-containing phase to interact with Hg^{2+} while maintaining the integrity of the beads during the sensing process. The immobilisation of AgNPs also facilitates visual observation of the colour change without requiring sophisticated instrumentation. As shown in Figure 7, the colour response became more apparent with increasing Hg^{2+} concentration, particularly after 30 min of exposure.

Overall, these findings demonstrate that the SA/AgNPs nanocomposite beads combine antibacterial activity and visual Hg^{2+} detection in a single biopolymer-based material. The use of sodium alginate as the matrix and the visible response to Hg^{2+} provide advantages for simple, potentially low-cost detection. Therefore, the SA/AgNPs nanocomposite beads show potential for preliminary or semi-quantitative monitoring of Hg^{2+} in aqueous samples.

Figure 8 presents a qualitative colourimetric evaluation of SA/AgNPs nanocomposite beads toward Sn^{2+}, Pb^{2+}, and Hg^{2+} ions at 100 ppm. The SA/AgNPs nanocomposite beads exhibited a distinct colour change from brown to white only after exposure to Hg^{2+}, whereas no noticeable colour change was observed in the presence of Sn^{2+} or Pb^{2+}. Similar selective colour responses of AgNP-based sensing systems toward Hg^{2+} have been reported in previous studies involving a broader range of competing metal ions, including Pb^{2+}, Cu^{2+}, Cd^{2+}, Zn^{2+}, Ni^{2+}, Co^{2+}, Fe^{2+}/Fe^{3+}, and other cations [20].

In these studies, Hg^{2+} produced a substantially stronger optical or visual response than the other tested ions, which was associated primarily with the redox interaction between Hg^{2+} and metallic Ag^0. In the present study, the absence of a visible response to Pb^{2+} and Sn^{2+} may similarly be related to their lower reduction potentials compared with the Ag^+/Ag^0 couple, making oxidation of Ag^0 by these ions thermodynamically less favourable. However, because the selectivity assessment in the present work was limited to two competing ions, the observed response should be regarded as preliminary evidence of preferential visual response toward Hg^{2+} rather than definitive selectivity. Further investigation using a broader range of potentially interfering ions is required to establish the selectivity of the SA/AgNPs nanocomposite beads more comprehensively [21].

4. Conclusion

Silver nanoparticle-loaded sodium alginate (SA/AgNPs) beads were successfully synthesised through a green approach using *Asplenium nidus* leaf extract. The formation of AgNPs was confirmed by UV–Vis and TEM analyses, while FTIR, SEM-EDS, and XRD characterisation supported the incorporation of the silver phase within the alginate matrix. The SA/AgNPs nanocomposite beads exhibited detectable antibacterial activity against *Escherichia coli* and *Staphylococcus aureus*, whereas pristine alginate beads showed no inhibitory activity under the tested conditions. The beads also demonstrated a qualitative visual colour change from brown to white after exposure to Hg^{2+} solutions, while no noticeable colour change was observed with Sn^{2+} and Pb^{2+} under the tested conditions. The observed colour change is likely associated with redox interactions between Hg^{2+} and Ag^{0}, accompanied by changes in the optical properties of the AgNPs. Overall, the findings demonstrate the potential of SA/AgNPs nanocomposite beads as a simple visual material for Hg^{2+} detection and as an antibacterial material. However, further quantitative sensing studies, including colourimetric analysis, sensitivity, detection limit, reproducibility, and real-sample validation, are required to establish their analytical performance and practical applicability.

Acknowledgment

The authors gratefully acknowledge the Institute for Research and Community Service (LPPM), University of Bengkulu, for providing financial support for this research through the Fundamental Research Grant scheme, under Contract No. 2941/UN.30.15/PT/2024.

References

[1] A. Sati, T. N. Ranade, S. N. Mali, H. K. Ahmad Yasin, A. Pratap, Silver Nanoparticles (AgNPs): Comprehensive Insights into Bio/Synthesis, Key Influencing Factors, Multifaceted Applications, and Toxicity—A 2024 Update, *ACS Omega*, 10, 8, (2025), 7549-7582 https://doi.org/10.1021/acsomega.4c11045

[2] N. Al-Gburi, A. Al-Hassnawi, L. A. Al-Bayati, Biosynthesis of Silver Nanoparticles and Their Roles in the Biomedical Field: A Review, *Medical Journal of Babylon*, 21, 3, (2024), 493-499 https://doi.org/10.4103/MJBL.MJBL_731_23

[3] Ankita Meher, Ashish Tandi, Srikanta Moharana, Subhendu Chakroborty, Susnata Sovalin Mohapatra, Arijit Mondal, Suddhasattya Dey, Prakash Chandra, Silver nanoparticle for biomedical applications: A review, *Hybrid Advances*, 6, (2024), 100184 https://doi.org/10.1016/j.hybadv.2024.100184

[4] M. Fahim, A. Shahzaib, N. Nishat, A. Jahan, T. A. Bhat, A. Inam, Green synthesis of silver nanoparticles: A comprehensive review of methods, influencing factors, and applications, *JCIS Open*, 16, (2024), 100125 https://doi.org/10.1016/j.jciso.2024.100125

[5] V. Budini, F. Bassetto, C. Scarpa, V. Vindigni, Silver nanoparticle dressing: The knowledge of advantages and limits improves the indications in clinical practice, *International Wound Journal*, 21, 4, (2024), e14872 https://doi.org/10.1111/iwj.14872

[6] H. Jangid, S. Singh, P. Kashyap, A. Singh, G. Kumar, Advancing biomedical applications: an in-depth analysis of silver nanoparticles in antimicrobial, anticancer, and wound healing roles, *Frontiers in Pharmacology*, 15, (2024), 1438227 https://doi.org/10.3389/fphar.2024.1438227

[7] S. Wahyudi, J. Abdul Aziz, F. Faizal, A. Bahtiar, Improved mercury ions (Hg^{2+}) detection by composite silver nanoparticles (AgNPs) and nitrogen - Sulfur co-doped carbon dots (N, S-CDs), *Results in Materials*, 21, (2024), 100551 https://doi.org/10.1016/j.rinma.2024.100551

[8] Irene Schiesaro, Luca Burratti, Carlo Meneghini, Ilaria Fratoddi, Paolo Prosposito, Joohyun Lim, Christina Scheu, Iole Venditti, Giovanna Iucci, Chiara Battocchio, Hydrophilic Silver Nanoparticles for Hg(II) Detection in Water: Direct Evidence for Mercury–Silver Interaction, *The Journal of Physical Chemistry C*, 124, 47, (2020), 25975-25983 https://doi.org/10.1021/acs.jpcc.0c06951

[9] Y. Yang, H. Qi, X. Hou, M. Gao, S. Gong, Recent Advances (2019–2025) in Mercury Ion Detection, *Critical Reviews in Analytical Chemistry*, 56, 6, (2025), 1912-1928 https://doi.org/10.1080/10408347.2025.2511136

[10] Muh S. Hakim, D. Hermayantiningsih, T. W. Manurung, M. Ariefin, M. Roil Bilad, Recent Progress on Colorimetric Sensor for Hg(II) Detection, *Jurnal Sains Materi Indonesia*, 27, 1, (2025), 1-10 https://doi.org/10.55981/jsmi.2025.8937

[11] M. Akhondi, A. H. Jafari, E. Jamalizadeh, Selective colorimetric detection of Hg^{II} using silver nanoparticles modified with Apple and Nigella Sativa seed extracts and β-Cyclodextrin, *Journal of Environmental Chemical Engineering*, 8, (2020), 103566 https://doi.org/10.1016/j.jece.2019.103566

[12] Monira Khatun, Ziasmin Khatun, Md. Rezaul Karim, Md. Rowshanul Habib, Md. Habibur Rahman, Md. Abdul Aziz, Green synthesis of silver nanoparticles using extracts of *Mikania cordata* leaves and evaluation of their antioxidant, antimicrobial and cytotoxic properties, *Food Chemistry Advances*, 3, (2023), 100386 https://doi.org/10.1016/j.focha.2023.100386

[13] E. Abada, A. Mashraqi, Y. Modafer, M. A. Al Abboud, A. El-Shabasy, Review green synthesis of silver nanoparticles by using plant extracts and their antimicrobial activity, *Saudi Journal of Biological Sciences*, 31, 1, (2024), 103877 https://doi.org/10.1016/j.sjbs.2023.103877

[14] M. R. Bindhu, M. Umadevi, G. A. Esmail, N. A. Al-Dhabi, M. V. Arasu, Green synthesis and characterization of silver nanoparticles from *Moringa oleifera* flower and assessment of antimicrobial and sensing properties, *Journal of Photochemistry and Photobiology B: Biology*, 205, (2020), 111836 https://doi.org/10.1016/j.jphotobiol.2020.111836

[15] Vishnu M. Sravanthi, S. Nirmala, Green synthesis of silver nanoparticles from *Vitex Altissima* extract: An in-vitro and in-silico evaluation of anti-inflammatory activity, *Sustainable Chemistry One*

World, 9, (2026), 100155 https://doi.org/10.1016/j.scowo.2025.100155

[16] A. M. Sivalingam, Green synthesis and characterization of silver nanoparticles (AgNPs) using *Bacopa monnieri* leaf extract photoluminescence (PL) profiling and applications of antioxidant, antimicrobial activity, *Inorganic Chemistry Communications*, 184, (2026), 115898 https://doi.org/10.1016/j.inoche.2025.115898

[17] S. S. Yudha, D. Notriawan, E. Angasa, T. Eka Suharto, J. Hendri, Y. Nishina, Green synthesis of silver nanoparticles using aqueous rinds extract of *Brucea javanica* (L.) Merr at ambient temperature, *Materials Letters*, 97, (2013), 181-183 https://doi.org/10.1016/j.matlet.2013.01.114

[18] S. Ahmed, M. Ahmad, B. L. Swami, S. Ikram, A review on plants extract mediated synthesis of silver nanoparticles for antimicrobial applications: A green expertise, *Journal of Advanced Research*, 7, 1, (2016), 17-28 https://doi.org/10.1016/j.jare.2015.02.007

[19] Jose Ruben Morones, Jose Luis Elechiguerra, Alejandra Camacho, Katherine Holt, Juan B. Kouri, Jose Tapia Ramírez, Miguel Jose Yacaman, The bactericidal effect of silver nanoparticles, *Nanotechnology*, 16, (2005), 2346 https://doi.org/10.1088/0957-4484/16/10/059

[20] S. Hajji, R. B. S. B. Salem, M. Hamdi, K. Jellouli, W. Ayadi, M. Nasri, S. Boufi, Nanocomposite films based on chitosan–poly(vinyl alcohol) and silver nanoparticles with high antibacterial and antioxidant activities, *Process Safety and Environmental Protection*, 111, (2017), 112-121 https://doi.org/10.1016/j.psep.2017.06.018

[21] S. Ediyilyam, B. George, S. S. Shankar, T. T. Dennis, S. Wacławek, M. Černík, Chitosan/Gelatin/Silver Nanoparticles Composites Films for Biodegradable Food Packaging Applications, *Polymers*, 13, 11, (2021), 1680 https://doi.org/10.3390/polym13111680

[22] Y. Xu, S. Li, X. Yue, W. Lu, Review of Silver Nanoparticles (AgNPs)-Cellulose Antibacterial Composites, *BioResources*, 13, 1, (2017), 2150-2170 https://doi.org/10.15376/biores.13.1.Xu

[23] F. Xie, Alginate-based nanocomposites for food preservation: Recent progress showcasing heightened material properties and functionalities, *Advanced Nanocomposites*, 1, 1, (2024), 248-274 https://doi.org/10.1016/j.adna.2024.07.002

[24] M. H. Abu Elella, A. M. Kamel, E. A. López-Maldonado, S. W. Uzondu, H. M. Abdallah, A review of recent progress in alginate-based nanocomposite materials for tissue engineering applications, *International Journal of Biological Macromolecules*, 297, (2025), 139840 https://doi.org/10.1016/j.ijbiomac.2025.139840

[25] F. Faghiri, F. Ghorbani, Colorimetric and naked eye detection of trace Hg^{2+} ions in the environmental water samples based on plasmonic response of sodium alginate impregnated by silver nanoparticles, *Journal of Hazardous Materials*, 374, (2019), 329-340 https://doi.org/10.1016/j.jhazmat.2019.04.052

[26] R. H. Wibowo, R. Setiawan, W. Darwis, S. Sipriyadi, R. Supriati, A. A. F. Ginting Sinisuka, Aktivitas Antibakteri dan Analisis Fitokimia Ekstrak Metanol dari Daun Paku Sarang Burung (*Asplenium nidus*), *Jurnal Ilmu Pertanian Indonesia*, 27, 3, (2022), 295-301 https://doi.org/10.18343/jipi.27.2.295

[27] Anupama Asthana, Renu Verma, Ajaya Kumar Singh, Md Abu Bin Hasan Susan, Rameshwar Adhikari, Silver Nanoparticle Entrapped Calcium-Alginate Beads for Fe(II) Removal via Adsorption, *Macromolecular Symposia*, 366, 1, (2016), 42-51 https://doi.org/10.1002/masy.201650045

[28] Adhitasari Suratman, Nurul Pramita, Pradiya Nadya Agasta, Dwi Ratih Purwaningsih, Agus Kuncaka, Eko Sri Kunarti, Atmanto Heru Wibowo, The effect of zeolite addition and freeze-drying method on alginat beads for controlled release fertilizer, *AIP Conference Proceedings*, 2237, 1, (2020), 020034 https://doi.org/10.1063/5.0005798